



## OPEN ACCESS

## EDITED BY

Waqar Ahsan,  
Jazan University, Saudi Arabia

## REVIEWED BY

Ratnamala A.,  
Indian Institute of Chemical Technology (CSIR),  
India

Flávio Figueira,  
University of Aveiro, Portugal

## \*CORRESPONDENCE

Ali Altharawi,  
✉ a.altharawi@psau.edu.sa

RECEIVED 15 February 2024

ACCEPTED 22 April 2024

PUBLISHED 13 May 2024

## CITATION

Altharawi A, Alqahtani SM, Aldakhil T and  
Ahmad I (2024), Microwave-assisted synthesis  
of novel Ti/BTB-MOFs as porous anticancer and  
antibacterial agents.

*Front. Chem.* 12:1386311.

doi: 10.3389/fchem.2024.1386311

## COPYRIGHT

© 2024 Altharawi, Alqahtani, Aldakhil and  
Ahmad. This is an open-access article  
distributed under the terms of the [Creative  
Commons Attribution License \(CC BY\)](#). The use,  
distribution or reproduction in other forums is  
permitted, provided the original author(s) and  
the copyright owner(s) are credited and that the  
original publication in this journal is cited, in  
accordance with accepted academic practice.  
No use, distribution or reproduction is  
permitted which does not comply with these  
terms.

# Microwave-assisted synthesis of novel Ti/BTB-MOFs as porous anticancer and antibacterial agents

Ali Altharawi<sup>1\*</sup>, Safar M. Alqahtani<sup>1</sup>, Taibah Aldakhil<sup>1</sup> and Irfan Ahmad<sup>2</sup>

<sup>1</sup>Department of Pharmaceutical Chemistry, College of Pharmacy, Prince Sattam Bin Abdulaziz University, Al-Kharj, Saudi Arabia, <sup>2</sup>Department of Clinical Laboratory Sciences, College of Applied Medical Science, King Khalid University, Abha, Saudi Arabia

Nano compounds, especially metal-organic frameworks (MOFs), have significant properties. Among the most important properties of these compounds, which depend on their specific surface area and porosity, are biological properties, such as anticancer and antibacterial properties. In this study, a new titanium/BTB metal-organic framework (Ti/BTB-MOF) was synthesized by using titanium nitrate and 1,3,5-Tris(4-carboxyphenyl)benzene (BTB) under microwave radiation. The structure of the synthesized Ti/BTB-MOF was characterized and confirmed using X-ray diffraction (XRD) patterns, X-ray photoelectron spectroscopy (XPS) analysis, Fourier transform infrared (FT-IR) spectra, energy-dispersive X-ray (EDAX) analysis mapping, scanning electron microscope (SEM) images, thermogravimetric analysis (TGA) curves, and Brunauer–Emmett–Teller (BET) analysis. The *in vitro* anticancer properties of Ti/BTB-MOF were evaluated using the MTT method against MG-63/bone cancer cells and A-431/skin cancer cells. The *in vitro* antibacterial activity was tested using the Clinical and Laboratory Standards Institute (CLSI) guidelines. In the anticancer activity, IC<sub>50</sub> (half-maximal inhibitory concentration) values of 152 µg/mL and 201 µg/mL for MG-63/bone cancer cells and A-431/skin cancer cells, respectively, were observed. In the antibacterial activity, minimum inhibitory concentrations (MICs) of 2–64 µg/mL were observed against studied pathogenic strains. The antimicrobial activity of Ti/BTB-MOF was higher than that of penicillin and gentamicin. Therefore, the synthesized Ti/BTB-MOF could be introduced as a suitable bioactive candidate.

## KEYWORDS

titanium-BTB metal-organic framework, anticancer agents, bone cancer cells, skin cancer cells, antibacterial agents

## 1 Introduction

Cancer is a common cause of human mortality (Turner et al., 2020). Although methods such as chemotherapy and laser are developing in the treatment of cancer, the reporting of compounds and the presence of new compounds with anticancer properties are still important (Dallavalle et al., 2020; Anduran et al., 2022; Melfi et al., 2023).

Bacteria, a common cause of disease in humans, can also cause the death of humans (Hussain et al., 2022). The excessive use of antibiotics to suppress these pathogenic agents has led to the resistance of some strains (Şen Karaman et al., 2020; Murugaiyan et al., 2022).

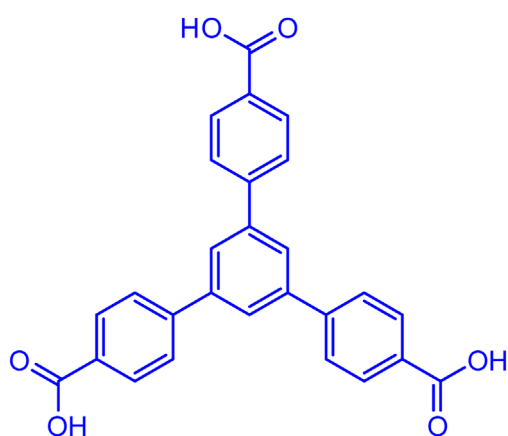


FIGURE 1  
Structure of 1,3,5-Tris(4-carboxyphenyl)benzene.

Providing new and innovative antibiotics is one way to deal with this problem (Terreni et al., 2021).

Nanotechnology and metal-organic frameworks (MOFs) have found a worthy place in medical science (Bieniek et al., 2021; de Alencar Filho et al., 2021). In MOFs, which are composed of ligands and metals, the most important roles of ligands are flexibility and the possibility of controlling the size and environment of the holes (Cai et al., 2021; Shen et al., 2021; Kumar et al., 2023). The properties of the ligand can be preserved in the final product and give the final product the properties of the ligand (Joyce et al., 2021; Sharifzadeh et al., 2021). 1,3,5-Tris(4-carboxyphenyl)benzene (Figure 1) is an organic compound consisting of four benzene rings and three carboxylic acid groups.

Some biological properties such as anticancer activity (Wani and Zargar, 2023) have been reported from 1,3,5-tris(4-carboxyphenyl)benzene, which is also called BTB. Because it has three carboxylic acid groups in its structure, BTB can coordinate with metals and create MOFs. Several metals, such as Cu (Ji et al., 2023), Fe (Viltres et al., 2024), and Zn (Choi et al., 2023) have been reported to synthesize with BTB to create MOFs. These MOFs have been used as electrochemical sensors (Ji et al., 2023), to eliminate antibiotics from water (Viltres et al., 2024), in the adsorption of cationic dyes (Li et al., 2021), in hydrocarbon adsorption/separation (Wang et al., 2020), etc.

Another main component of MOFs is the metal. Metals, like ligands, can maintain their properties in MOF compounds (Qiu et al., 2020; Seidi et al., 2020; He et al., 2021). The d-block elements of the periodic table have a high ability as metals in the synthesis of MOF compounds (Roslan and Aris, 2023). Titanium, whose position is in Group 4 and d-block elements of the periodic table, has been used as a catalyst in the synthesis of chemicals (Samhitha et al., 2022) and as an antibacterial (Aslam et al., 2021), anticancer (Samhitha et al., 2022), and antioxidant agent (Muthuvel et al., 2021).

In this study, a microwave-assisted method was used to synthesize Ti/BTB-MOF nanostructures. This route is fast, controllable, and economical compared to other methods. In addition, this effective method has produced Ti/BTB-MOF samples with favorable physicochemical properties, which have affected the antibacterial applications of the final compound. Another advantage of this study is the synthesis of Ti/BTB-

MOFs as novel anticancer and antibacterial candidates that can be used in other biological fields due to their practical properties.

## 2 Materials, methods, and characterization

### 2.1 Materials

The titanium (IV) nitrate (99.9%) was obtained from Sigma-Aldrich. The 1,3,5-Tris(4-carboxyphenyl)benzene (98%) was obtained from TCI Chemicals.

The bone cancer cells (MG-63), skin cancer cells (A-431), and the pathogenic bacterial strains studied were obtained from the American Type Culture Collection (ATCC).

### 2.2 Methods

#### 2.2.1 Titanium/BTB metal-organic framework (Ti/BTB-MOF)

Using ultrasonic, 1.4 mmol 1,3,5-benzene-tri-4-carboxyphenyl (BTB) was dispersed in 20 mL double distilled water. A-1 mmol aliquot of titanium (IV) nitrate was added to the mixture and stirred for 10 min (800 rpm) at room temperature. The mixture was subjected to microwave irradiation for 15 min (power of 350 W) (Bashar et al., 2022). The synthesized titanium/BTB-MOF was washed three times with EtOH and then three times with H<sub>2</sub>O. For drying, the synthesized Ti/BTB-MOF was placed under vacuum in an oven at 100°C for 3 h.

#### 2.2.2 Anticancer tests

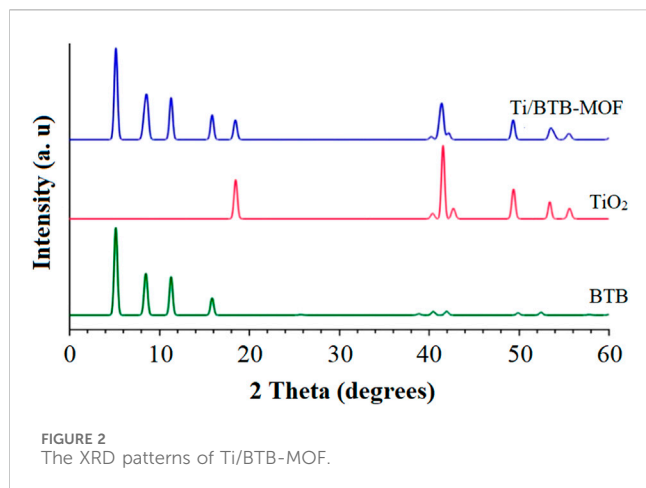
The *in vitro* anticancer activity of Ti/BTB-MOF was investigated using MTT (3-[4,5-dimethylthiazol-2-yl]-2,5 diphenyl tetrazolium bromide) assay protocols (Rhodes, 1996; Moghaddam-manesh et al., 2021; Alkhatami et al., 2023). In the evaluation and tests, concentrations of 5 µg/mL, 10 µg/mL, 20 µg/mL, 40 µg/mL, 80 µg/mL, 160 µg/mL, and 320 µg/mL of titanium/BTB-MOF were prepared and treated separately with MG-63/bone cancer cells and A-431/skin cancer cells for 24 h and 48 h.

#### 2.2.3 Antibacterial tests

*In vitro* antibacterial tests of Ti/BTB-MOF were investigated using the Clinical and Laboratory Standards Institute (CLSI) and antimicrobial susceptibility testing methods (Etemadi et al., 2016; Moghaddam-Manesh et al., 2020; Terreni et al., 2021). The antibacterial activity of titanium/BTB-MOF was investigated against the pathogenic strains ATCC 33809 (*Vibrio fluvialis*), ATCC 25729 (*Rhodococcus equi*), ATCC 29178 (*Streptococcus iniae*), ATCC 9610 (*Yersinia enterocolitica*), ATCC 13313 (*Shigella dysenteriae*), and ATCC 19115 (*Listeria monocytogenes*).

### 2.3 Characterization and equipment

X-ray diffraction (XRD) patterns, X-ray photoelectron spectroscopy (XPS) analysis, Fourier transform infrared (FT-IR) spectra, energy-dispersive X-ray (EDAX) analysis mapping, scanning



electron microscope (SEM) images, thermogravimetric analysis (TGA) curves, and Brunauer–Emmett–Teller (BET) analysis were used to characterize and confirm the structure of Ti/BTB-MOF. The equipment used for analysis were a DW-XRD-Y3000 (XRD), a SPECS Phoibos 150 (UHV-XPS), a Thermo Nicolet Avatar 360 (FT-IR), a TESCAN MIRA3 (EDAX, EDAX mapping, and

SEM), a TA Instruments SDT-Q600 (TGA), and a BELSORP mini II (BET).

In antibacterial activity tests, the required concentration of the studied strains was prepared using a Jenway 7315 UV/Visible spectrophotometer.

In anticancer activity tests, a KERN OCM 161 inverted microscope was used to count cancer cells, and an Accuris MR9610 SmartReader UV-Vis (115 V) was used to measure absorbance.

## 3 Results

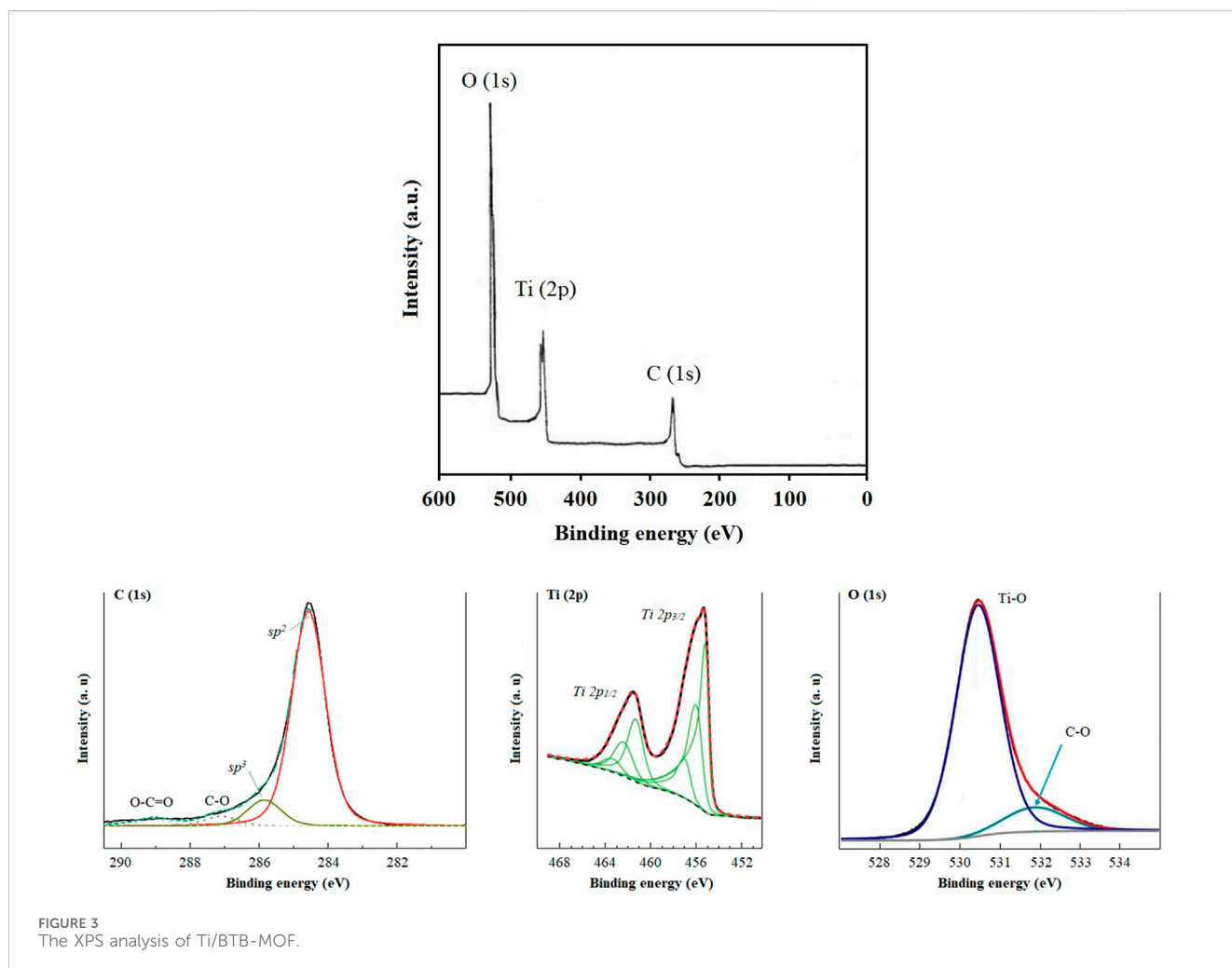
### 3.1 Ti/BTB-MOF synthesis results

The XRD pattern of Ti/BTB-MOF is given in [Figure 2](#).

In the XRD pattern of Ti/BTB-MOF, plates [011], [002], [121], [222], and [132] were observed at  $2\theta$ .

In the XPS analysis of Ti/BTB-MOF ([Figure 3](#)), binding energies of 283 eV, 458 eV, 464 eV, and 532 eV were observed.

In the FT-IR spectrum related to the Ti/BTB-MOF, as shown in [Figure 4](#), absorptions at  $655\text{ cm}^{-1}$ ,  $1,150\text{ cm}^{-1}$ ,  $1,420\text{ cm}^{-1}$ ,  $1,710\text{ cm}^{-1}$ , and  $2,900\text{ cm}^{-1}$  were observed.



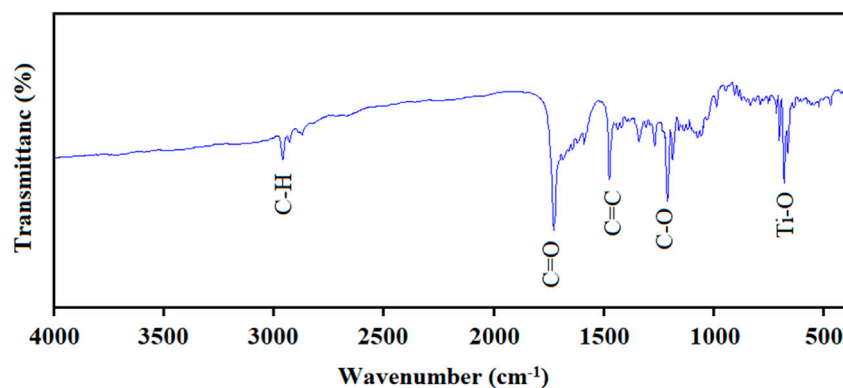


FIGURE 4  
The FT-IR spectrums of Ti/BTB-MOF.

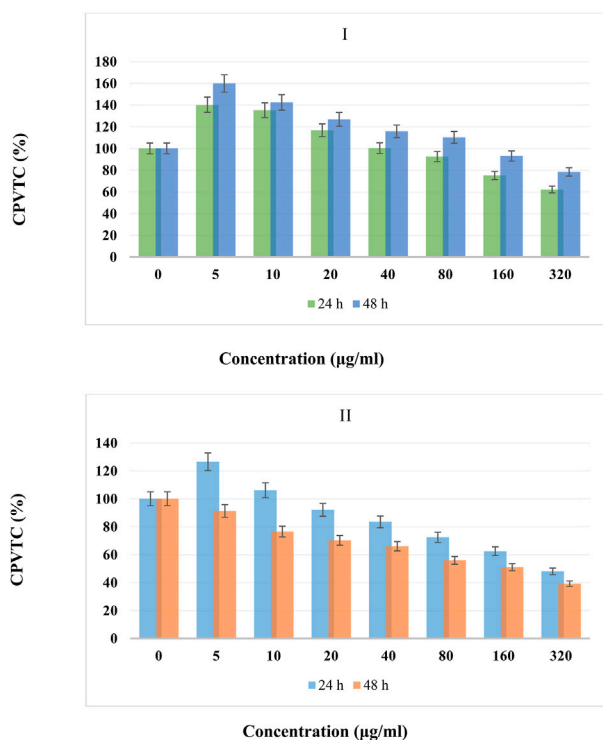


FIGURE 5  
The CPVTC of BTB (I) and Ti/BTB-MOF (II) against skin cancer cells, ( $n = 3$ )  $\pm$  SD.

Figure 5 shows the thermal stability of the final product. Two areas of basic weight loss were observed in the TGA curve in the regions of 350°C and 480°C.

The nitrogen adsorption and desorption curves of Ti/BTB-MOF are shown in Figure 6.

The obtained BET, mean pore diameter, and Barrett–Joyner–Halenda (BJH) pore volume are given in Table 1.

## 3.2 Anticancer test results

### 3.2.1 Anti-bone cancer cells

The cell proliferation and viability compared to control (CPVTC) of different concentrations of BTB (I) and Ti/BTB-MOF (II) against bone cancer cells at temperatures of 24 h and 48 h are given in Figure 7.

Based on the obtained results, at 24 h, the CPVTC for concentrations of 5 µg/mL, 10 µg/mL, 20 µg/mL, 40 µg/mL, 80 µg/mL, 160 µg/mL, and 320 µg/mL of Ti/BTB-MOF were obtained as 114%, 99% 85%, 73%, 62%, 54%, and 42% compared to the control, respectively.

At 48 h, the CPVTC for concentrations of 5 µg/mL, 10 µg/mL, 20 µg/mL, 40 µg/mL, 80 µg/mL, 160 µg/mL, and 320 µg/mL of Ti/BTB-MOF were obtained as 85%, 71%, 66%, 59%, 52%, 43%, and 27% compared to the control, respectively.

For BTB at 24 h, the CPVTC for concentrations of 5 µg/mL, 10 µg/mL, 20 µg/mL, 40 µg/mL, 80 µg/mL, 160 µg/mL, and 320 µg/mL were obtained as 167%, 150% 131%, 120%, 109%, 95%, and 81% compared to the control, respectively.

At 48 h, the CPVTC for concentrations of 5 µg/mL, 10 µg/mL, 20 µg/mL, 40 µg/mL, 80 µg/mL, 160 µg/mL, and 320 µg/mL of BTB were obtained as 155%, 142%, 127%, 103%, 99%, 80%, and 66% compared to the control, respectively.

### 3.2.2 Anti-skin cancer cells

The CPVTC of different concentrations of BTB (I) and Ti/BTB-MOF (II) against skin cancer cells at 24 h and 48 h are given in Figure 8.

Based on the obtained results, at 24 h, the CPVTC for concentrations of 5 µg/mL, 10 µg/mL, 20 µg/mL, 40 µg/mL, 80 µg/mL, 160 µg/mL, and 320 µg/mL of Ti/BTB-MOF were obtained as 126%, 106% 92%, 83%, 72%, 62%, and 48% compared to the control, respectively.

At 48 h, the CPVTC for concentrations of 5 µg/mL, 10 µg/mL, 20 µg/mL, 40 µg/mL, 80 µg/mL, 160 µg/mL, and 320 µg/mL of Ti/BTB-MOF were obtained as 91%, 76%, 70%, 65%, 55%, 51%, and 39% compared to the control, respectively.

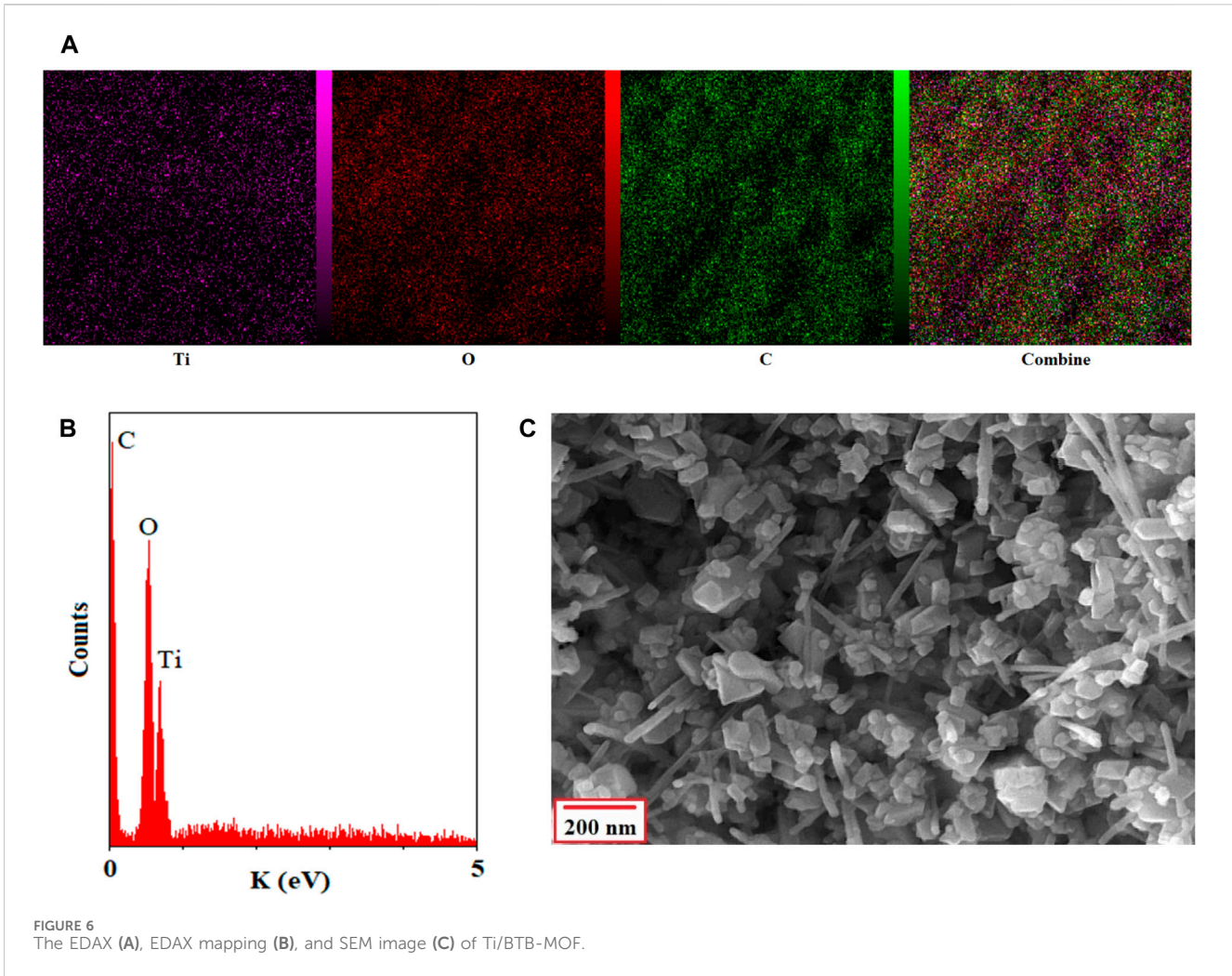


TABLE 1 BET, Barrett–Joyner–Halenda (BJH) pore volume, and mean pore diameter of Ti/BTB-MOF.

BET (m <sup>3</sup> /g)	BJH pore volume (cm <sup>3</sup> /g)	Mean pore diameter (nm)
35	0.42	1.36

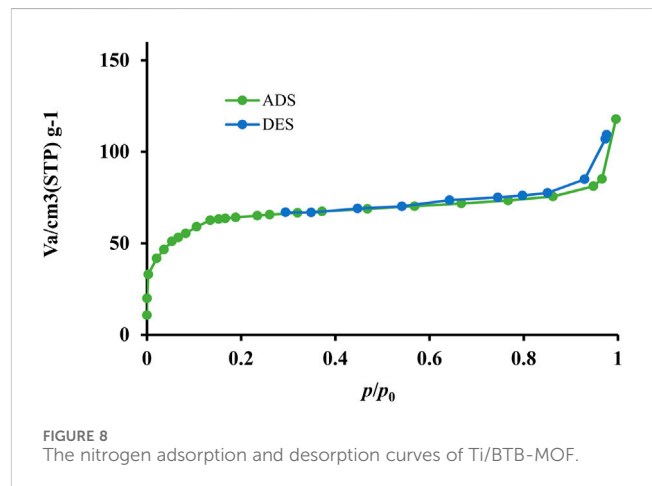
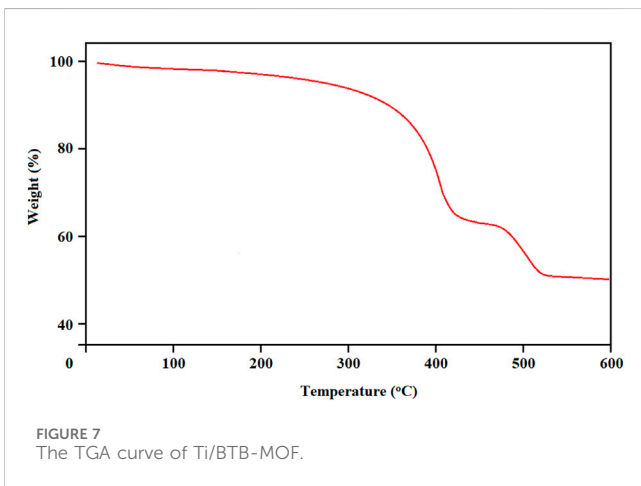




TABLE 2 Antibacterial activity of Ti/BTB-MOF (mean, n = 3).

Compound strain	BTB			Ti/BTB-MOF			Penicillin			Gentamicin		
	MIC $\mu\text{g}/\text{mL}$	MBC $\mu\text{g}/\text{mL}$	IZD mm	MIC $\mu\text{g}/\text{mL}$	MBC $\mu\text{g}/\text{mL}$	IZD mm	MIC $\mu\text{g}/\text{mL}$	MBC $\mu\text{g}/\text{mL}$	IZD mm	MIC $\mu\text{g}/\text{mL}$	MBC $\mu\text{g}/\text{mL}$	IZD mm
ATCC 33809	-	-	-	64	128	15.37	-	-	-	-	-	-
ATCC 25729	64	128	17.01	16	32	17.93	4	8	19.63	2	4	20.42
ATCC 29178	128	256	13.25	2	4	20.64	2	4	18.75	4	16	18.31
ATCC 9610	-	-	-	32	64	14.92	-	-	-	-	-	-
ATCC 13313	16	32	16.71	4	16	19.31	32	64	15.27	2	4	22.43
ATCC 19115	32	64	19.49	2	4	20.08	1	2	20.75	-	-	-

For BTB at 24 h, the CPVTC for concentrations of 5  $\mu\text{g}/\text{mL}$ , 10  $\mu\text{g}/\text{mL}$ , 20  $\mu\text{g}/\text{mL}$ , 40  $\mu\text{g}/\text{mL}$ , 80  $\mu\text{g}/\text{mL}$ , 160  $\mu\text{g}/\text{mL}$ , and 320  $\mu\text{g}/\text{mL}$  were obtained as were obtained as 159%, 142%, 126%, 115%, 110%, 93%, and 78% compared to the control, respectively.

At 48 h, the CPVTC for concentrations of 5  $\mu\text{g}/\text{mL}$ , 10  $\mu\text{g}/\text{mL}$ , 20  $\mu\text{g}/\text{mL}$ , 40  $\mu\text{g}/\text{mL}$ , 80  $\mu\text{g}/\text{mL}$ , 160  $\mu\text{g}/\text{mL}$ , and 320  $\mu\text{g}/\text{mL}$  of BTB were obtained as 140%, 135%, 116%, 100%, 92%, 75%, and 62% compared to the control, respectively.

### 3.2.3 Antibacterial test results

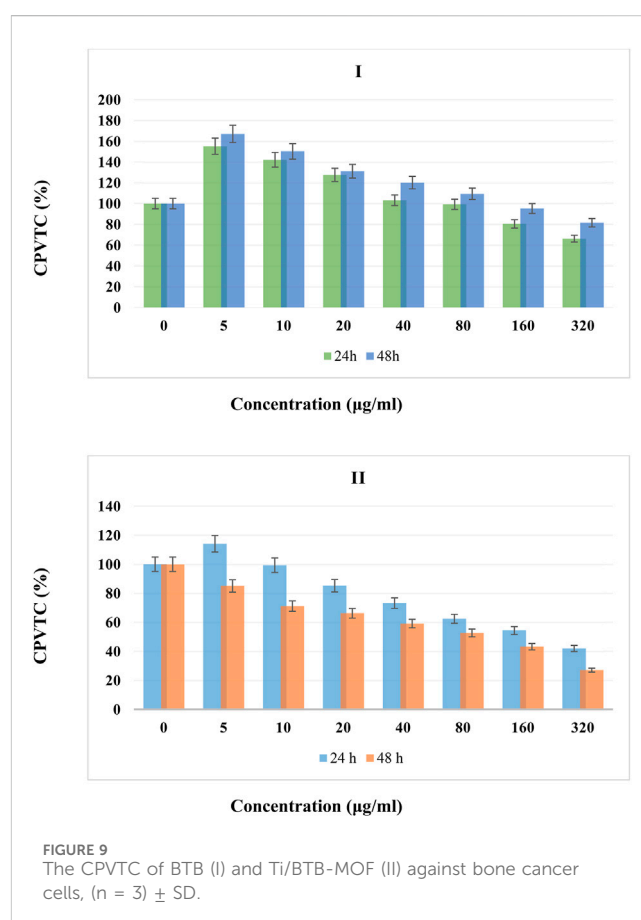
The antibacterial activities of BTB, Ti/BTB-MOF, penicillin, and gentamicin were investigated. The minimum inhibitory concentration (MIC), minimum bactericidal concentration (MBC), and inhibitory zone diameter (IZD) were tested and reported. The tests were repeated three times, and the results, which are the average of three repetitions, are shown in Table 2.

## 4 Discussion

### 4.1 Synthesis of Ti/BTB-MOF

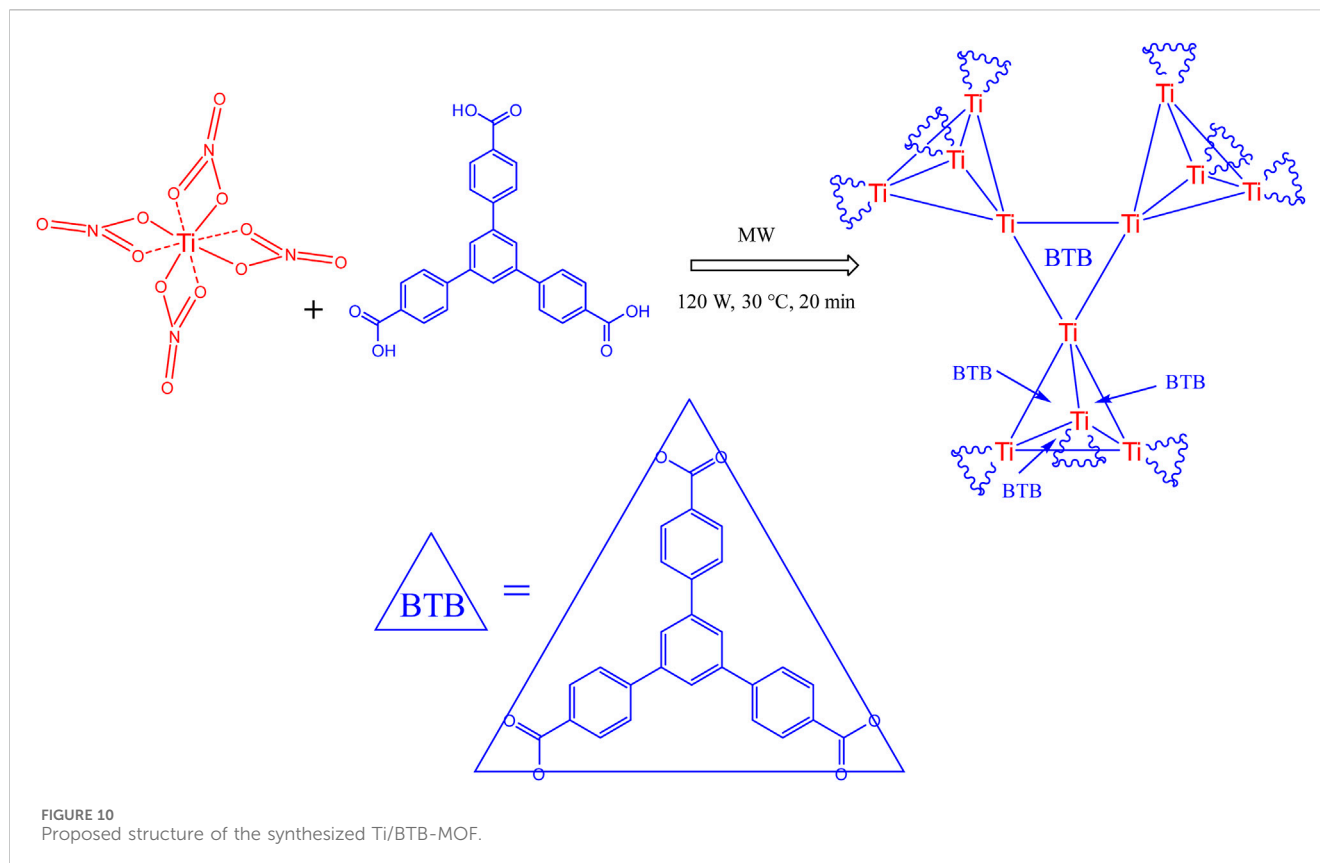
In this study, a novel Ti/BTB-MOF was synthesized using titanium (IV) nitrate and 1,3,5-Tris(4-carboxyphenyl)benzene under microwave irradiation. The purpose of using the microwave method is to provide optimal conditions for forming MOF nanostructures with desirable properties such as small particle size distribution, desirable thermal stability, and good textural properties. The mechanism of formation of MOF nanostructures by using a microwave-assisted method is developed in this study based on previous literature (Choi et al., 2008; Couzon et al., 2022; Fernández-Andrade et al., 2023).

The most important factor in the formation of products using the microwave-assisted method is the heating process. The basis of this process is the interaction between the electrical component of microwaves and polar compounds. Due to the unique characteristics of these waves when heating during chemical reactions, microwaves have been widely used to synthesize nanomaterials, MOFs, organic compounds, etc. In this study, microwave irradiation with a power of 350 W was used as the reaction condition. A literature review showed that a power of 350 W leads to a temperature close to 130°C (Xiaokang et al., 2020).



The structure of the final product was predicted and confirmed using the XRD patterns, XPS analysis, EDAX analysis, and EDAX mapping. Then, other characteristics of nanoparticles were investigated and studied using the SEM images, TGA curves, and the BET technique.

The XRD pattern of the final product (Figure 2) was similar to the XRD pattern reported for the crystal structure of titanium nanoparticles (Gómez-Avilés et al., 2020). The XRD patterns of the samples indicate that the nanostructures developed in this study have a higher percentage of crystalline phases than previous reports (Gómez-Avilés et al., 2020). This difference can be related to the efficient effects of the microwave-assisted route on the crystalline properties of the final product.



Using XRD data and the Debye–Scherrer equation, the synthesized Ti/BTB-MOF was 68 nm (Holzwarth and Gibson, 2011).

In the XPS analysis of Ti/BTB-MOF (Figure 3), the binding energies related to carbon (1s-283 eV) (Oh et al., 2013; Susi et al., 2015; Tudino et al., 2020), titanium (2p<sub>1/2</sub>-458 eV, and 2p<sub>3/2</sub>-464 eV) (Shvab et al., 2017), and oxygen (1s-532 eV) (Tudino et al., 2020) were observed.

The absorptions observed in the FT-IR spectrum (Figure 4) near 655 cm<sup>-1</sup>, 1,150 cm<sup>-1</sup>, 1,420 cm<sup>-1</sup>, 1,710 cm<sup>-1</sup>, and 2,900 cm<sup>-1</sup> were related to Ti-O (Al-Amin et al., 2016), C-O (Alkhatami et al., 2023), C=C (Alkhatami et al., 2023), C=O (Akhavan-Sigari et al., 2022), and C-H (Ahmad et al., 2022), respectively. The BTB has three carboxylic acid groups, but the broad band due to O-H groups (near 3,200–3,500 cm<sup>-1</sup>) was not observed in the spectrum of the final product.

Based on the EDAX and EDAX mapping of Ti/BTB-MOF (Figure 9A,B), titanium, carbon, and oxygen were observed in the structure of the final product.

Therefore, the structure of Figure 10 can be predicted for the novel Ti/BTB-MOF by using XRD patterns, which indicate the presence of titanium nanoparticles in Ti/BTB-MOF structure, the XPS analysis, which indicates the binding energies of carbon, titanium, and oxygen in the final product, FT-IR spectrum, which indicates the absorption of the elements of the raw materials and the bonding of Ti-O and the absence of O-H in the product, and EDAX, EDAX mapping, which proves the presence of carbon, titanium, and oxygen in the final product.

SEM, TGA, and BET were used to obtain other characteristics of the Ti/BTB-MOF.

The SEM image of the final product proves its uniformity (Figure 9C) and its nano-size. Uniform morphology and nano-size are parameters that depend on the synthesis method of nanoparticles (Yaqoob et al., 2020). Therefore, it can be concluded that the technique of synthesizing Ti/BTB-MOF using microwave radiation is suitable for this study.

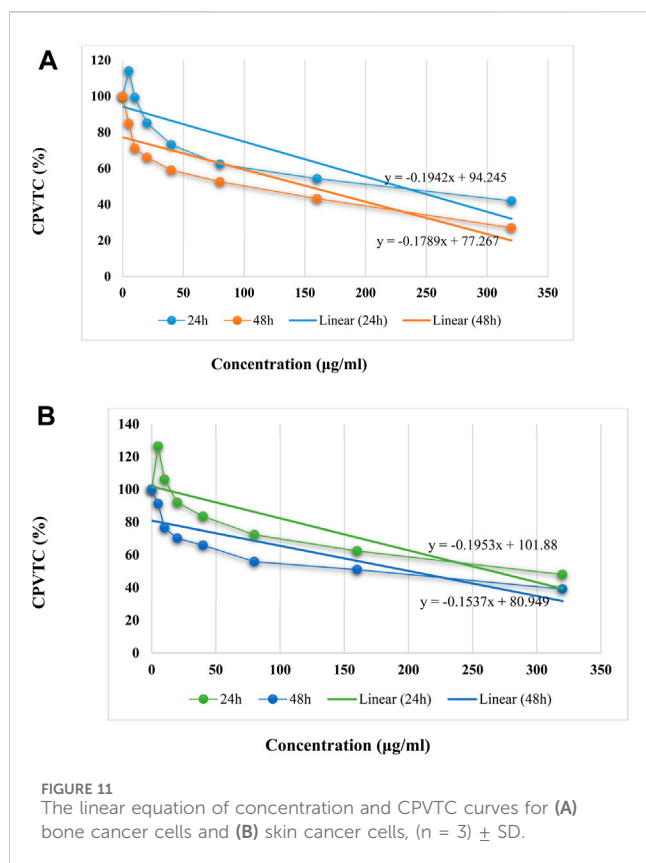
Based on Figure 5, the weight loss observed at 350°C can be attributed to the destruction of BTB, and the weight loss observed at 480°C can be attributed to the destruction of the complex.

Using nitrogen adsorption and desorption curves (Figure 6) and the BET technique, the specific surface area for Ti/BTB-MOF was obtained as 35 m<sup>2</sup>/g. In nanoparticles, the specific surface area depends on the synthesizing technique (Sajid and Płotka-Wasyłka, 2020). The high specific surface area indicates that this study used an appropriate synthesis method.

## 4.2 Anticancer activity of Ti/BTB-MOF

Figures 7, 8 show the best effectiveness and lowest CPVTC anticancer activity against bone and skin cancer cells at 48 h and 320 µg/mL of Ti/BTB-MOF.

In anticancer activity, the IC<sub>50</sub> values of Ti/BTB-MOF against bone cancer cells and skin cancer cells were calculated by using the linear equation of cell proliferation and viability and concentration curve (Figure 11). The IC<sub>50</sub> values against bone cancer cells were



228 µg/mL (24 h) and 152 µg/mL (48 h), and the  $IC_{50}$  values against skin cancer cells were 266 µg/mL (24 h) and 201 µg/mL (48 h).

For BTB, the  $IC_{50}$  values against bone cancer cells were 453.73 µg/mL (24 h) and 354 µg/mL (48 h), and the  $IC_{50}$  values against skin cancer cells were 448 µg/mL (24 h) and 337 µg/mL (48 h).

Comparing the anticancer results of BTB and Ti/BTB-MOF indicated that the anticancer activity of Ti/BTB-MOF was higher than that of BTB. The reason can be attributed to the nanostructure that is formed and the presence of titanium in the final product.

Based on previous results, the  $IC_{50}$  values for doxorubicin, which is known as the standard drug against bone and skin cancer cells, have been reported to be close to 50 µg/mL (Rezadoost et al., 2019), which is about 1/3 of the values observed for Ti/BTB-MOF. However, because Ti/BTB-MOF has additional properties, such as its antibacterial activities, the synthesized compound is useful and important.

In the anticancer activities of Ti/BTB-MOF, the  $p$ -values of the  $IC_{50}$  values at 24 h and 48 h were calculated, and the results are given in Table 3.

The  $p$ -value results of the investigation of anticancer activity against bone and skin cancer cells indicated that concentrations

were a critical parameter at 24 and 48 h. By increasing the time and increasing the nanoparticle concentration, the contact of cancer cells with the Ti/BTB-MOF increases and leads to an increase in its anticancer properties. As previous studies have suggested, increasing the specific surface area increases biological activities (Cui and Zhu, 2021), so here, too, the high specific surface area of Ti/BTB-MOF leads to an increase in contact with cancer cells and increased anticancer properties. Other factors, such as the biological properties of the BTB (Wani and Zargar, 2023) and Ti (Aslam et al., 2021; Samhitha et al., 2022) in the Ti/BTB-MOF structure also influence the anticancer activity.

### 4.3 Antibacterial activity of Ti/BTB-MOF

In antibacterial evaluations, as shown in Table 2, MIC values against *V. fluvialis*, *R. equi*, *S. iniae*, *Y. enterocolitica*, *S. dysenteriae*, and *L. monocytogenes* were obtained as 128 µg/mL, 32 µg/mL, 4 µg/mL, 64 µg/mL, 16 µg/mL, and 4 µg/mL, respectively. The Ti/BTB-MOF against *S. iniae* had the highest effectiveness. Tests were performed on penicillin and gentamicin, well-known antibiotics on the market. The results showed that penicillin and gentamicin are ineffective on *V. fluvialis* and *Y. enterocolitica*, but significant effectiveness of Ti/BTB-MOF was observed, which is another unique capability of synthesized Ti/BTB-MOF. The antibacterial results of BTB against the studied strains were also higher than those of gentamicin in some strains, such as *L. monocytogenes*. However, the BTB results were generally lower than Ti/BTB-MOF, which can be attributed to the formed nanostructure and the presence of titanium.

The high antimicrobial properties of nanoparticles against the studied strains can also be due to their high specific surface area, leading to more contact and, therefore, more destruction (Khezerlou et al., 2018; Cui and Zhu, 2021). In addition, other factors, such as the biological properties of the BTB (Wani and Zargar, 2023) and Ti (Aslam et al., 2021; Samhitha et al., 2022) in Ti/BTB-MOF structure, also influence anticancer activity.

## 5 Conclusion

By using microwave radiation, novel titanium/1,3,5-Tris(4-carboxyphenyl)benzene metal-organic frameworks (Ti/BTB-MOFs) were synthesized. The structure of synthesized Ti/BTB-MOF was predicted using XRD, XPS, FT-IR, EDAX, and EDAX mapping. The Ti/BTB-MOF was characterized using SEM, TGA, and BET. The Ti/BTB-MOF had thermal stability up to 350°C. The specific surface area of Ti/BTB-MOF was 35 m<sup>2</sup>/g. The 68-nm particle size was another feature of the Ti/BTB-MOF. These characteristics proved that the use of microwave radiation was suitable for the synthesis of Ti/BTB-MOF. The anticancer properties of nanoparticles against bone and skin cancer cells

TABLE 3 The  $p$ -values of the  $IC_{50}$  values of Ti/BTB-MOF against bone cancer cells and skin cancer cells.

Cancer cell	$p$ -value 24 h (µg/mL)	$p$ -value 48 h (µg/mL)
Bone cancer cells	0.002	0.000
Skin cancer cells	0.001	0.001



were evaluated. In the investigation,  $IC_{50}$  values for bone and skin cancer cells were obtained as 152  $\mu\text{g}/\text{mL}$  and 201  $\mu\text{g}/\text{mL}$ , respectively. The antibacterial properties of the synthesized Ti/BTB-MOF were also evaluated, and MIC, MBC, and IZD were reported. The antibacterial activity of Ti/BTB-MOF was compared with trade drugs, and on some of the studied strains, Ti/BTB-MOF had better inhibition than the drugs.

## Data availability statement

The original contributions presented in the study are included in the article/Supplementary Material; further inquiries can be directed to the corresponding author.

## Author contributions

AA: writing–review and editing, writing–original draft, project administration, conceptualization, methodology. SA: writing–review and editing, supervision, investigation, visualization. TA: writing–review and editing, writing–original draft, formal analysis, validation. IA: writing–review and editing, writing–original draft, resources.

## References

- Ahmad, I., Jasim, S. A., Yasin, G., Al-Qargholi, B., and Hammid, A. T. (2022). Synthesis and characterization of new 1, 4-dihydropyran derivatives by novel Ta-MOF nanostructures as reusable nanocatalyst with antimicrobial activity. *Front. Chem.* 10, 967111. doi:10.3389/fchem.2022.967111
- Akhavan-Sigari, R., Zeraati, M., Moghaddam-Manesh, M., Kazemzadeh, P., Hosseinzadegan, S., Chauhan, N. P. S., et al. (2022). Porous Cu-MOF nanostructures with anticancer properties prepared by a controllable ultrasound-assisted reverse micelle synthesis of Cu-MOF. *BMC Chem.* 16, 10. doi:10.1186/s13065-022-00804-2
- Al-Amin, M., Dey, S. C., Rashid, T. U., Ashduzzaman, M., and Shamsuddin, S. M. (2016). Solar assisted photocatalytic degradation of reactive azo dyes in presence of anatase titanium dioxide. *Int. J. Latest Res. Eng. Technol.* 2, 14–21.
- Alkhatami, A. G., Khaled Younis Albahady, W., Jawad, M. A., Ramadan, M. F., Alsaraf, K. M., Riyad Muedii, Z. a.-H., et al. (2023). Hydrogel assistant synthesis of new Ti-MOF cross-linked oxidized pectin and chitosan with anti-breast cancer properties. *Front. Mater.* 10, 1264529. doi:10.3389/fmats.2023.1264529
- Anduran, E., Dubois, L. J., Lambin, P., and Winum, J.-Y. (2022). Hypoxia-activated prodrug derivatives of anti-cancer drugs: a patent review 2006–2021. *Expert Opin. Ther. Pat.* 32, 1–12. doi:10.1080/13543776.2021.1954617
- Aslam, M., Abdullah, A. Z., and Rafatullah, M. (2021). Recent development in the green synthesis of titanium dioxide nanoparticles using plant-based biomolecules for environmental and antimicrobial applications. *J. Industrial Eng. Chem.* 98, 1–16. doi:10.1016/j.jiec.2021.04.010
- Bashar, B. S., Kareem, H. A., Hasan, Y. M., Ahmad, N., Alshehri, A., Al-Majidi, K., et al. (2022). Application of novel Fe<sub>3</sub>O<sub>4</sub>/Zn-metal organic framework magnetic nanostructures as an antimicrobial agent and magnetic nanocatalyst in the synthesis of heterocyclic compounds. *Front. Chem.* 10, 1014731. doi:10.3389/fchem.2022.1014731
- Bieniek, A., Terzyk, A. P., Wiśniewski, M., Roszek, K., Kowalczyk, P., Sarkisov, L., et al. (2021). MOF materials as therapeutic agents, drug carriers, imaging agents and biosensors in cancer biomedicine: recent advances and perspectives. *Prog. Mater. Sci.* 117, 100743. doi:10.1016/j.pmatsci.2020.100743
- Cai, G., Yan, P., Zhang, L., Zhou, H.-C., and Jiang, H.-L. (2021). Metal-organic framework-based hierarchically porous materials: synthesis and applications. *Chem. Rev.* 121, 12278–12326. doi:10.1021/acs.chemrev.1c00243
- Choi, I. H., Gu, J. M., Kim, H. C., Kim, Y., and Huh, S. (2023). Gas sorption properties of a new Zn-BTB metal-organic framework with permanent porosity. *Bull. Korean Chem. Soc.* 44, 780–787. doi:10.1002/bkcs.12707
- Choi, J.-S., Son, W.-J., Kim, J., and Ahn, W.-S. (2008). Metal-organic framework MOF-5 prepared by microwave heating: factors to be considered. *Microporous Mesoporous Mater.* 116, 727–731. doi:10.1016/j.micromeso.2008.04.033
- Couzon, N., Ferreira, M., Duval, S., El-Achari, A., Campagne, C., Loiseau, T., et al. (2022). Microwave-assisted synthesis of porous composites MOF-textile for the protection against chemical and nuclear hazards. *ACS Appl. Mater. Interfaces* 14, 21497–21508. doi:10.1021/acsami.2c03247
- Cui, R., and Zhu, F. (2021). Ultrasound modified polysaccharides: a review of structure, physicochemical properties, biological activities and food applications. *Trends Food Sci. Technol.* 107, 491–508. doi:10.1016/j.tifs.2020.11.018
- Dallavalle, S., Dobričić, V., Lazzarato, L., Gazzano, E., Machuqueiro, M., Pajeva, I., et al. (2020). Improvement of conventional anti-cancer drugs as new tools against multidrug resistant tumors. *Drug Resist. Updat.* 50, 100682. doi:10.1016/j.drug.2020.100682
- de Alencar Filho, J. M. T., Sampaio, P. A., Silva De Carvalho, I., Rocha Da Silva, A., Pereira, E. C. V., Araujo E Amariz, L., et al. (2021). Metal organic frameworks (MOFs) with therapeutic and biomedical applications: a patent review. *Expert Opin. Ther. Pat.* 31, 937–949. doi:10.1080/13543776.2021.1924149
- Etemadi, Y., Shiri, A., Eshghi, H., Akbarzadeh, M., Saadat, K., Mozafari, S., et al. (2016). Synthesis, characterisation, and *in vitro* antibacterial evaluation of a new class of 2-substituted-4-methyl-7, 8-dihydro-5H-pyrimido [4, 5-d] thiazolo [3, 2-a] pyrimidines. *J. Chem. Res.* 40, 600–603. doi:10.3184/174751916x14737838285904
- Fernández-Andrade, K. J., Fernández-Andrade, A. A., Zambrano-Intriago, L. Á., Arteaga-Perez, L. E., Alejandro-Martin, S., Baquerizo-Crespo, R. J., et al. (2023). Microwave-assisted MOF@ biomass layered nanomaterials: characterization and applications in wastewater treatment. *Chemosphere* 314, 137664. doi:10.1016/j.chemosphere.2022.137664
- Gómez-Avilés, A., Muelas-Ramos, V., Bedia, J., Rodriguez, J. J., and Belver, C. (2020). Thermal post-treatments to enhance the water stability of NH<sub>2</sub>-MIL-125 (Ti). *Catalysts* 10, 603. doi:10.3390/catal10060603
- He, T., Kong, X.-J., and Li, J.-R. (2021). Chemically stable metal-organic frameworks: rational construction and application expansion. *Accounts Chem. Res.* 54, 3083–3094. doi:10.1021/acs.accounts.1c00280
- Holzwarth, U., and Gibson, N. (2011). The Scherrer equation versus the Debye-Scherrer equation. *Nat. Nanotechnol.* 6, 534. doi:10.1038/nnano.2011.145
- Hussain, H. H., Ibraheem, N. T., Al-Rubaey, N. K. F., Radhi, M. M., Hindi, N. K. K., and Al-Jubori, R. H. K. (2022). A review of airborne contaminated microorganisms associated with human diseases. *Med. J. Babylon* 19, 115–122. doi:10.4103/mjbl.mjbl\_20\_22
- Ji, X.-X., Liu, Y.-L., Chang, X.-Y., Li, R.-L., Ye, F., Yang, L., et al. (2023). An electrochemical sensor derived from Cu-BTB MOF for the efficient detection of diflubenzuron in food and environmental samples. *Food Chem.* 428, 136802. doi:10.1016/j.foodchem.2023.136802

## Funding

The author(s) declare that financial support was received for the research, authorship, and/or publication of this article. The authors extend their appreciation to Prince Sattam bin Abdulaziz University for funding this research work through the project number (PSAU/2023/03/27184).

## Conflict of interest

The authors declare that the research was conducted in the absence of any commercial or financial relationships that could be construed as a potential conflict of interest.

## Publisher's note

All claims expressed in this article are solely those of the authors and do not necessarily represent those of their affiliated organizations, or those of the publisher, the editors, and the reviewers. Any product that may be evaluated in this article, or claim that may be made by its manufacturer, is not guaranteed or endorsed by the publisher.

- Joyce, K., Fabra, G. T., Bozkurt, Y., and Pandit, A. (2021). Bioactive potential of natural biomaterials: identification, retention and assessment of biological properties. *Signal Transduct. Target. Ther.* 6, 122. doi:10.1038/s41392-021-00512-8
- Khezerlou, A., Alizadeh-Sani, M., Azizi-Lalabadi, M., and Ehsani, A. (2018). Nanoparticles and their antimicrobial properties against pathogens including bacteria, fungi, parasites and viruses. *Microb. Pathog.* 123, 505–526. doi:10.1016/j.micpath.2018.08.008
- Kumar, S., Chauhan, C., Kumar, R., Kalra, N., Saini, A., Sharma, S., et al. (2023). Concomitant role of metal clusters and ligands in the synthesis and control of porosity in metal-organic frameworks: a literature review. *Results Chem.* 6, 101206. doi:10.1016/j.rechem.2023.101206
- Li, H., Gao, K., Mo, B., Meng, Q., Li, K., Wu, J., et al. (2021). Construction of porous 2D MOF nanosheets for rapid and selective adsorption of cationic dyes. *Dalton Trans.* 50, 3348–3355. doi:10.1039/d0dt04143b
- Melfi, F., Carradori, S., Mencarelli, N., Campestre, C., Gallorini, M., Di Giacomo, S., et al. (2023). Natural products as a source of new anticancer chemotypes. *Expert Opin. Ther. Pat.* 33, 721–744. doi:10.1080/13543776.2023.2265561
- Moghaddam-Manesh, M., Beyzaei, H., Heidari Majid, M., Hosseinzadegan, S., and Ghazvini, K. (2021). Investigation and comparison of biological effects of regioselectively synthesized thiazole derivatives. *J. Heterocycl. Chem.* 58, 1525–1530. doi:10.1002/jhet.4278
- Moghaddam-Manesh, M., Ghazanfari, D., Sheikhsosseini, E., and Akhgar, M. (2020). Synthesis, characterization and antimicrobial evaluation of novel 6'-Amino-spiro [indeno [1, 2-b] quinoxaline [1, 3] dithiine]-5'-carbonitrile derivatives. *Acta Chim. Slov.* 67, 276–282. doi:10.17344/acsi.2019.5437
- Murugaiyan, J., Kumar, P. A., Rao, G. S., Iskandar, K., Hawser, S., Hays, J. P., et al. (2022). Progress in alternative strategies to combat antimicrobial resistance: focus on antibiotics. *Antibiotics* 11, 200. doi:10.3390/antibiotics11020200
- Muthuvel, A., Said, N. M., Jothibas, M., Gurushankar, K., and Mohana, V. (2021). Microwave-assisted green synthesis of nanoscaled titanium oxide: photocatalyst, antibacterial and antioxidant properties. *J. Mater. Sci. Mater. Electron.* 32, 23522–23539. doi:10.1007/s10854-021-06840-3
- Oh, D. X., Shin, S., Lim, C., and Hwang, D. S. (2013). Dopamine-mediated sclerotization of regenerated chitin in ionic liquid. *Materials* 6, 3826–3839. doi:10.3390/ma6093826
- Qiu, T., Liang, Z., Guo, W., Tabassum, H., Gao, S., and Zou, R. (2020). Metal-organic framework-based materials for energy conversion and storage. *ACS Energy Lett.* 5, 520–532. doi:10.1021/acsenerylett.9b02625
- Rezadoost, M. H., Kumleh, H. H., and Ghasempour, A. (2019). Cytotoxicity and apoptosis induction in breast cancer, skin cancer and glioblastoma cells by plant extracts. *Mol. Biol. Rep.* 46, 5131–5142. doi:10.1007/s11033-019-04970-w
- Rhodes, R. (1996). Cell titer 96 non-radioactive cell proliferation assays and cytotoxic 96 non-radioactive cytotoxicity assay. *Promega Notes* 59, 50–51.
- Roslan, M. Q. J., and Aris, A. Z. (2023). Review: removal of endocrine-disrupting compounds (EDCs) from water bodies using metal-organic frameworks (MOFs) with diverse linkers incorporating periodic elements and demonstrating high adsorption efficiency. *J. Environ. Chem. Eng.* 11, 111345. doi:10.1016/j.jece.2023.111345
- Sajid, M., and Płotka-Wasyłka, J. (2020). Nanoparticles: synthesis, characteristics, and applications in analytical and other sciences. *Microchem. J.* 154, 104623. doi:10.1016/j.microc.2020.104623
- Samhitha, S. S., Raghavendra, G., Quezada, C., and Bindu, P. H. (2022). Green synthesized TiO<sub>2</sub> nanoparticles for anticancer applications: mini review. *Mater. Today Proc.* 54, 765–770. doi:10.1016/j.matpr.2021.11.073
- Seidi, F., Jouyandeh, M., Taghizadeh, M., Taghizadeh, A., Vahabi, H., Habibzadeh, S., et al. (2020). Metal-organic framework (MOF)/epoxy coatings: a review. *Materials* 13, 2881. doi:10.3390/ma13122881
- Şen Karaman, D., Ercan, U. K., Bakay, E., Topaloğlu, N., and Rosenholm, J. M. (2020). Evolving technologies and strategies for combating antibacterial resistance in the advent of the postantibiotic era. *Adv. Funct. Mater.* 30, 1908783. doi:10.1002/adfm.201908783
- Sharifzadeh, Z., Berijani, K., and Morsali, A. (2021). Chiral metal-organic frameworks based on asymmetric synthetic strategies and applications. *Coord. Chem. Rev.* 445, 214083. doi:10.1016/j.ccr.2021.214083
- Shen, Y., Pan, T., Wang, L., Ren, Z., Zhang, W., and Huo, F. (2021). Programmable logic in metal-organic frameworks for catalysis. *Adv. Mater.* 33, 2007442. doi:10.1002/adma.202007442
- Shvab, R., Hryha, E., and Nyborg, L. (2017). Surface chemistry of the titanium powder studied by XPS using internal standard reference. *Powder Metall.* 60, 42–48. doi:10.1080/00325899.2016.1271092
- Susi, T., Pichler, T., and Ayala, P. (2015). X-ray photoelectron spectroscopy of graphitic carbon nanomaterials doped with heteroatoms. *Beilstein J. Nanotechnol.* 6, 177–192. doi:10.3762/bjnano.6.17
- Terreni, M., Taccani, M., and Pregnotato, M. (2021). New antibiotics for multidrug-resistant bacterial strains: latest research developments and future perspectives. *Molecules* 26, 2671. doi:10.3390/molecules26092671
- Tudino, T. C., Nunes, R. S., Mandelli, D., and Carvalho, W. A. (2020). Influence of dimethylsulfoxide and dioxygen in the fructose conversion to 5-hydroxymethylfurfural mediated by glycerol's acidic carbon. *Front. Chem.* 8, 263. doi:10.3389/fchem.2020.00263
- Turner, M. C., Andersen, Z. J., Baccarelli, A., Diver, W. R., Gapstur, S. M., Pope Iii, C. A., et al. (2020). Outdoor air pollution and cancer: an overview of the current evidence and public health recommendations. *CA a cancer J. Clin.* 70, 460–479. doi:10.3322/caac.21632
- Viltres, H., Phung, V., Gupta, N., Morera-Boado, C., Sheikhlar, A. M., Rajabzadeh, A. R., et al. (2024). Rapid and effective antibiotics elimination from water by Fe-BTB MOF: an insight into adsorption mechanism. *J. Mol. Liq.* 397, 124105. doi:10.1016/j.molliq.2024.124105
- Wang, X., Wang, X., Zhang, X., Fan, W., Li, Q., Jiang, W., et al. (2020). A stable interpenetrated Zn-MOF with efficient light hydrocarbon adsorption/separation performance. *Cryst. Growth & Des.* 20, 5670–5675. doi:10.1021/acs.cgd.0c00925
- Wani, T. A., and Zargar, S. (2023). Molecular spectroscopy evidence of 1, 3, 5-tris (4-carboxyphenyl) benzene binding to DNA: anticancer potential along with the comparative binding profile of intercalation via modeling studies. *Cells* 12, 1120. doi:10.3390/cells12081120
- Xiaokang, W., Lyng, J. G., Brunton, N. P., Cody, L., Jacquier, J.-C., Harrison, S. M., et al. (2020). Monitoring the effect of different microwave extraction parameters on the recovery of polyphenols from shiitake mushrooms: comparison with hot-water and organic-solvent extractions. *Biotechnol. Rep.* 27, e00504. doi:10.1016/j.btre.2020.e00504
- Yaqoob, A. A., Umar, K., and Ibrahim, M. N. M. (2020). Silver nanoparticles: various methods of synthesis, size affecting factors and their potential applications—a review. *Appl. Nanosci.* 10, 1369–1378. doi:10.1007/s13204-020-01318-w